CHEOPS-GOME

Algorithm Theoretical Basis Document

Level 0 to 1 Processing Update

Author: Sander Slijkhuis
Doc.No.: CH-TN-DLR-GO-0003
Issue: 1/B
Date: 5 June 2006

Deutsches Zentrum für Luft- und Raumfahrt e.V. - DLR
Institut für Methoden der Fernerkundung - IMF
Oberpfaffenhofen
Germany

Change Record

Issue	*Rev.*	*Date*	*Page*	*Description*
1		17.09.2004	all	New document
1	A	19.10.2004	page 12	Different data format for BSDF
1	B	05.06.2006	11 14 16 16 18 all	Fixed offset and error removed Division by correction factor, not multiplication Numerical values of parameter matrix c Value of $\Delta\lambda_{GDF}$ Reference to SRON degradation study Removal of TBDs and minor text edits

Tabel of Contents

1 Introduction

1.1 Project Scope

The Global Ozone Monitoring Experiment (GOME) was originally conceived as a scaled-down version of SCIAMACHY, with very similar mission objectives [R1] [R2]. It was given fast-track development status by ESA [R3], and was launched on 21 April 1995 on board the second European Remote Sensing Satellite (ERS-2). It has 4 spectral channels covering the range 240-790 nm, and is a nadir-only instrument.

The GOME Data Processor (GDP) was developed and implemented at DLR with scientific support of several institutions [R4], notably University of Heidelberg, University of Bremen (IFE), SAO, KNMI, ISAO-CNR, RAL, Max-Planck-Institut für Chemie/Mainz. GDP became operational in July 1996, with calibrated Earth-shine spectra and retrieved total O_3 columns the main products generated on a routine basis (Level 1, Level 2 products, respectively). Since then the GDP has been further developed by DLR-MF using inputs from SRON, BISA, and several of the above institutions [R6][R7].

As scientific algorithms were developed to perform retrieval of height-resolved O_3 profiles from GOME data, it became apparent that the standard GDP Level 1 product needed improvements to cope with the enhanced requirements on instrument calibration posed by profile retrieval. Several groups performed their own post-processing of Level 1 data to fulfil their own requirements; a public domain software package was made available by KNMI [R17].

In the framework of the CHEOPS-GOME project: “Climatology of Height-resolved Earth Ozone and Profiling Systems for GOME” ESA has undertaken an effort to incorporate the necessary improvements in GOME calibration in the official Level 1 data.

1.2 Document Purpose and Scope

This Algorithm Theoretical Basis Document (ATBD) describes the algorithms required for the post-processing of the GOME Level 1b data product, to obtain Level 1 data fulfilling the requirements for Ozone Profile retrieval within the CHEOPS-GOME project.

This ATBD provides detailed physical descriptions of algorithms which may be integrated into the GDP extraction software [R5][R7]. The function of the extraction processing is to convert the binary level 1b product, consisting of raw instrument signals (“binary units”) plus calibration constants plus partly calibrated data, into an ascii file containing the calibrated radiance (or in case of solar observations, into calibrated irradiance).

In this document we will provide algorithms dealing with correction of the degradation in reflectance, with improving the diffuser calibration and the polarisation algorithm, and with improving the Peltier offset correction (implicitly including a better correction of straylight in channel 1a). As the scope of this project is to improve the GOME level 1 data for the purpose of Ozone profile retrieval, which in this project will be performed using channels 1 and 2 of GOME, the algorithms will primarily deal with these two channels. E.g., improving the degradation correction or improving the polarisation correction will not be considered for channels 3 and 4.

1.3 Abbreviations and Acronyms

ADC	Analogue to Digital Converter
ATBD	Algorithm Theoretical Basis Document
BISA	Belgium Institute for Space Aeronomy (Brussels/Uccle, B)
BSDF	Bi-directional Scattering Distribution Function
BU	Binary Unit
CU	Calibration Unit of the GOME instrument
DFD	Deutsches Fernerkundungsdatenzentrum
DLR	Deutsches Zentrum für Luft- und Raumfahrt e.V.
DLR-MF	Institut für Methodik der Fernerkundung, DLR
DOAS	Differential Optical Absorption Spectroscopy
DPM/PDL	Detailed Processing Model / Parameter Data List
ERS	European Remote Sensing Satellite
ESA	European Space Agency
ESTEC	European Space Centre of Technology
FOV	Field of View
FPA	Focal Plane Assembly (GOME detector block)
FPN	Fixed Pattern Noise
FWHM	Full Width Half Maximum
GDF	General Distribution Function
GDP	GOME Data Processor
GOME	Global Ozone Monitoring Experiment
GSAG	GOME Scientific Advisory Group
IFE	Institut für Fernerkundung der Universität Bremen (D)
IFOV	Instantaneous Field of View
ILOS	Instantaneous Line of Sight
I/ODD	Input/Output Data Definition
IT	Integration Time
KNMI	Koninklijk Nederlands Meteorologisch Instituut (De Bilt, NL)
LUT	Look-up Table
MME	Mueller Matrix Element
PCA	Polarisation Correction Algorithm
PMD	Polarisation Measurement Device
PPG	Pixel-to-Pixel Gain
RAL	Rutherford Appleton Laboratory (Oxford, UK)
SAA	Southern Atlantic Anomaly
SAO	Smithsonian Astrophysical Observatory (Cambridge, USA)
SCIAMACHY	Scanning Imaging Absorption Spectrometer for Atmospheric Chartography
SLS	Spectral Light Source
SMR	Sun Mean Reference
SRON	Space Research Organisation of The Netherlands (Utrecht, NL)
SM	Scan Mirror
SZA	Solar Zenith Angle
TNO-TPD	Technisch Physische Dienst (Delft, NL)
TOA	Top of Atmosphere
TOMS	Total Ozone Mapping Spectrometer
UV	ultra-violet
VIS	Visible

2 GOME Background Information

2.1 Instrument Characteristics

GOME is a medium-resolution UV-VIS spectrometer, fed by a scan mirror which enables across-track scanning in Nadir, as well as sideways viewing for instrument characterisation measurements using the Moon; this scan mirror can also be directed towards internal calibration sources or towards a diffuser plate for calibration measurements using the Sun.

GOME contains 4 optical channels which focus the spectrum on linear detector arrays of 1024 pixels each, and 3 Polarisation Measurements Devices (PMDs) containing a photodiode, which measure linearly polarised intensity in one direction. These PMD measurements are performed over a broad wavelength band (100 - 200 nm), but at higher spatial resolution which allows a mapping of the cloud coverage on the ground.

The four main channels provide continuous spectral coverage of the wavelengths between 240-790 nm with a spectral resolution between ~0.2 nm (at 240 nm) and ~0.4 nm (at 790 nm). The spectra are formed by reflection gratings. Since the reflecting properties of these gratings are strongly polarisation-dependent, the intensity calibration of GOME has to take account of the polarisation of the incoming light, using information from the PMDs. Channels 1 and 2 are electronically split in two subchannels each. This allows for different integration times in each subchannel, to cope with the large dynamic range in intensity of the earthshine radiance (due to ozone absorption in the UV). The channel characteristics are listed in Table 1; we list here the useful illuminated spectral range - on a low intensity level the channels extend somewhat further.

The PMDs measure intensity polarised parallel to the spectrometer’s slit. If we define the plane of polarisation to be coincident with the local meridian plane (through viewing direction and through nadir; this coincides with the scanning plane - see Figure 1) then the PMDs measures the $-Q$ Stokes Intensity. In the GOME calibration algorithm, the polarisation is described using the fraction of light polarised parallel to the spectrometer’s slit. This polarisation parameter is denoted p and is a simple transformation of the Stokes fraction Q/I given by: $p = 0,5 \cdot (1 - Q/I)$

Channel nr	*Spectral Range [nm]*	*Resolution [nm]*	*Comment*
1a	237 – 307	0.16 – 0.19	< 265 nm not used for O3 profile retrieval
1b	307 – 314	0.16	
2a	311 – 312	0.25	not useable in later years
2b	312 – 405	0.16 – 0.25	
3	410 – 600	0.27 – 0.35	
4	610 – 790	0.35	
PMD 1	290 – 400	–	IR leak
PMD 2	400 – 600	–	
PMD 3	570 – 900	–	

Table 1: Useful channel boundaries and PMD ranges.

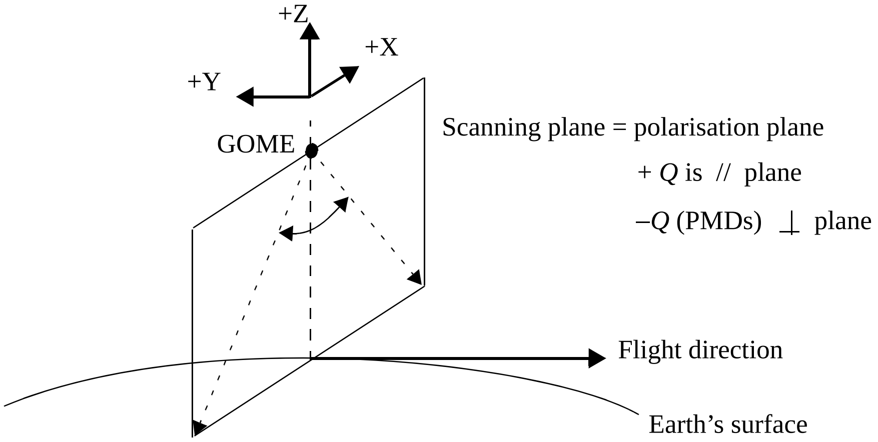

Figure 1: Definition of polarisation plane for PMDs

A basic concept in the operation of the GOME instrument, which is also reflected in the structure of the level 0 and level 1 data products, is that of the '**Scan**'. A Scan is defined as a time interval of 6 seconds, which during nominal scientific observations comprises one scan cycle (regular forward scan + fast flyback). In the default measuring mode, the scan mirror sweeps in 4.5 seconds from East to West (at the descending, sunlight part of the orbit; from West to East otherwise) followed by a faster flyback of 1.5 seconds back to the 'East' position. The default swath width of the scan is 960 km (which enables global coverage of the Earth's surface within 3 days) and the scan mirror speed is adjusted such that, despite the projection effect, the ground is scanned at constant speed. The height of the field-of-view (FOV) is ~40 km which is matched with the spacecraft velocity, such that each scan closely follows the ground coverage of the previous one.

The actual integration time used (and thus the ground pixel size) depends on the light intensity. Channel 1a has as default an integration time of 12 seconds; under low light conditions this is extended to 60 seconds. All other Channels have as default an integration time of 1.5 seconds; under low light conditions this is extended to 6 seconds.

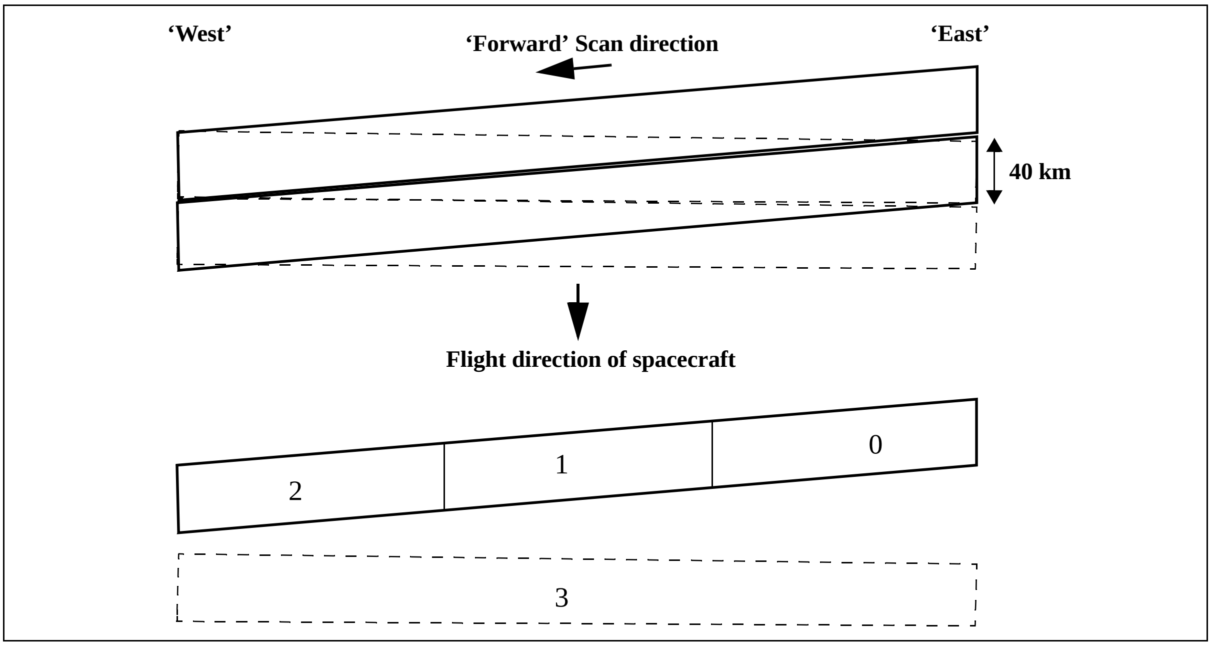

Figure 2: Scan pattern in default scan mode
(solid line: forward scan; dashed line: flyback). Each subset pixel (0-3) lasts 1.5 seconds.

In the largest part of the orbit, the ground coverage will lie directly below the satellite. However, this would leave the polar regions uncovered because of the inclination of the orbit. To be able to probe the chemically interesting atmospheric regions around the pole, a 'polar viewing' mode can be implemented which has the centre of the scan offset by 46^o (~800 km). It is envisaged to have polar viewing either at the south pole or at the north pole, such that the pole is observed in local spring time ('ozone hole' conditions).

Several calibration quantities depend on scan angle, and thus on 'pixel type' (i.e. East, Centre, West, or Backscan). Only for Channel 1a the measurements are averaged over scan angle, and here the scan angle dependence needs not to be taken into account (except in 'polar view' mode).

2.2 The generic calibration equation

The generic expression for the signal detected by each detector pixel, as function of the incident radiation and as function of the instrument characteristics, can be written as:

$$S_i = I(\lambda_i) \cdot T(\lambda_i) \cdot Q_i + SS_i + DS_i \quad \text{with}$$

S_i measured signal at detector pixel i

λ_i wavelength of detector pixel i

$I(\lambda_i)$ incident radiation as function of wavelength

$T(\lambda_i)$ optical transmission function of instrument as function of wavelength

Q_i detector efficiency (including conversion to 'binary units') of detector pixel i

SS_i straylight at detector pixel i (depending on all signals in the channel)

DS_i dark signal of detector pixel i

which by inversion yields the expression for the retrieved atmospheric intensity (on the Level 1b product given in units of photons/(s.cm2.sr.nm) for Earth-shine measurements c.q. photons/(s.cm2.nm) for the Sun measurements):

$$I(\lambda_i) = \frac{S_i - SS_i - DS_i}{T(\lambda_i) \cdot Q_i}$$

Instrument calibration comprises the determination of all quantities (except S_i) in the right-hand side of this equation. The quantities in the denominator deserve special attention, since they are in practice varying with time due to:

- wavelength shifts
- general degradation of the optics
- degradation of detector pixels
- varying interference patterns on detector (e.g. build-up of thin ice layers).

The latter problem is called Etaloning [R11]. The changes in etalon manifest themselves as a changing sinusoidal pattern, with typically 3-10 waves per channel.

When correcting the Response function of the instrument, $T(\lambda_i) \cdot Q_i$, for wavelength shifts we encounter the problem that only its wavelength-dependent part must be shifted and not its pixel-dependent part (the wavelength-dependent part is formed by the transmission of the optics and the quantum efficiency of the detector material; the pixel-dependent part is formed by pixel size and possible radiation damages to pixels).

Changes in instrument response function other than the above are usually caused by a gradual degradation in optics or electronics. This degradation must be monitored by scientific analysis of the data set. Such changes in instrument response may in the calibration equation accounted for by so-called monitoring factors.

An additional complication is that the instrument response function depends on the polarisation state of the incoming light. This is implemented as a polarisation correction factor, applied to the response function measured for unpolarised light. The polarisation state of the incoming light is determined for each measured channel signal, using the PMD-detector measurements recorded during the integration time of the channel signal.

Taking all of the above effects into account, we can rewrite the generic calibration equation as:

$$I(\lambda_i) = \frac{S_i - SS_i - DS_i}{c_{pol}(\lambda_i, p_t(\lambda_i)) \cdot (R_{0,i}/PPG_{0,i})(\lambda_i) \cdot PPG_{t,i} \cdot m_t(\lambda_i) \cdot E_t(\lambda_i)}$$

where subscript 0 denotes the quantity at a reference time $t = 0$ and subscript t denotes the quantity at the time of measurement, and

$(R_{0,i}/PPG_{0,i})(\lambda_i)$ smooth part of radiance response function as function of wavelength, for unpolarised input

$c_{pol}(\lambda_i, p_t(\lambda_i))$ polarisation correction factor as function of wavelength and input polarisation

$PPG_{t,i}$ pixel-to-pixel part of response function at detector pixel i

$m_t(\lambda_i)$ degradation monitoring factor as function of wavelength

$E_t(\lambda_i)$ etalon change as function of wavelength

The above equation is valid for the atmospheric measurements. For the observation of the Sun there is additionally a diffuser plate (plus auxiliary optics) in the light path. The scattering properties of the diffuser plate depend both on the elevation angle of the incident beam (which is a function of time in the orbit) and on its azimuth angle (which is a function of time of the year); this 2-dimensional dependency is expressed in the bi-directional scattering function (*BSDF*) of the diffuser. Noting that the sunlight is unpolarised, the generic calibration equation then takes the form:

$$I_{Sun}(\lambda_i) = \frac{S_i - SS_i - DS_i}{BSDF_0(\lambda_i) \cdot m_{BSDF,t}(\lambda_i) \cdot (R_{0,i}/PPG_{0,i})(\lambda_i) \cdot PPG_{t,i} \cdot m_t(\lambda_i) \cdot E_t(\lambda_i)}$$

In ozone profile retrieval, we effectively use the sun-normalised intensity. Here, the terms $E_t(\lambda_i)$, $PPG_{t,i}$ and $(R_{0,i}/PPG_{0,i})(\lambda_i)$ fall out of the equation, so that the relevant remaining calibrations are for straylight (for each measurement), dark signal (in principle for each orbit, but due to Peltier crosstalk for each measurement), BSDF (for each day depending on solar azimuth angle), polarisation correction (for each radiance measurement), and for degradation in the reflectance.

The latter term is given by:

$$m_{BSDF,t}(\lambda_i) \cdot \frac{m_t(\lambda_i)_{Sun}}{m_t(\lambda_i)_{Earth}} \quad (1)$$

where the right-hand term represents the scan-angle dependence of the degradation.

Note, that the degradation correction which can currently be applied in the GDP extraction software (version 2.21), describes the term $m_{BSDF,\,t}(\lambda_i) \cdot m_t(\lambda_i)_{Sun}$. It is applied there to Solar irradiances and Earthshine radiances equally, neglecting the scan angle dependence, and assuming that degradation of the diffuser itself is negligible.

2.3 Level 1b Processing in the GDP extraction software

In order to put the algorithms described in this ATBD into perspective, we provide here the current sequence of signal processing for the GDP Extraction software, taken from [R7].

Apply Dark Signal

Subtract the correct dark signal spectrum from the measured spectrum.

Correction for FPA noise

Applies a correction factor for interference from the Peltier coolers on the Focal Plane Assembly.

Apply PPG

Applies the calibration constants for PPG to the measurement spectrum.

Apply Spectral Calibration Parameters

Calculates for each detector pixel its wavelength [nm] from the spectral calibration parameters.

Apply Straylight Correction

Uses pre-flight straylight characteristics (uniform straylight fraction and ghost intensities/widths) to calculate the straylight spectrum and subtracts it from the measurements.

Apply BSDF

Uses measurements of the Sun over the diffuser to calculate a (daily) Sun Mean Reference spectrum, where the irradiance is calibrated via the BSDF function of the diffuser. This calibrated irradiance is stored on the Level 1b product; in the extraction software only a unit conversion may be applied. In addition, there is a switch to apply an azimuth correction based on data from an external ‘degradation file’ (option -e or -f)

Apply Radiance Response

Perform the absolute radiometric calibration of the detector signals, including the calculation of the radiometric accuracy.

Apply Polarisation Correction

The 7 Fractional Polarisation Values are interpolated to wavelength. This is partly done using modified spline interpolation (Akima), partly using a parameterisation of the polarisation curve in the UV. From the interpolated polarisation values, a polarisation correction factor is derived for and applied to each channel array detector pixel of the Earth-shine measurements.

Calculation of errors)

Calculates the precision of the measured spectrum, and its accuracy, using errors on keydata and fractional polarisation from the Level 1b product.

3 Algorithms Detailed Description

3.1 Apply Residual Offset Correction

This correction is based on the CHEOPS-GOME study of signal background [R20]. The results of this study are obtained by using a method where the correction is made after the correction for straylight.

One may argue that, from a point of principle, it might be better to apply this correction *before* the calculation of straylight, since straylight correction uses the amount of photons in the channel, which may be obtained from the signal corrected for dark signal and corrected for Peltier offset. Note, that this would have been difficult to implement in the study, because the effectiveness of the correction can only be assessed after straylight correction, which then would have to be made by hand. As the straylight correction is based on the total intensity in the channel, and as the number of counts in the Peltier correction is small compared to the total intensity, the error made in the straylight correction is expected to be negligible.

Therefore, we stick to the procedure described in [R20] and implement the correction *after* the correction for straylight.

The offset is only corrected for long integration times, which limits it to channel 1a. Here we use the signal of the “straylight band 1a” just before the beginning of the nominal band 1a.

1. The algorithm uses the first 20 pixels of the straylight band 1a, starting at pixel 206 in channel 1 (we count from 0 in this description).
2. These are sorted w.r.t. signal intensity.
3. The intensity of the *k*-th sorted pixel is used to further correct the measurements.
   We take $k = 9$ (i.e. the 10th sorted pixel when counting from 1)

The lowest intensity is not used because of noise, higher intensities are not used because they may be affected by cosmic rays or by straylight. The study indicates that a fixed offset (in BU) is present between this method and the KNMI method. Therefore, it may be that an offset has to be added to correct for a systematic effect. The magnitude of this offset needs to be established using validation on the basis of Ozone profile retrievals. As initial offset, we will take the mean difference between “average a” and “average d” in Table 1 from [R20], since we are here using “method a” from the study, while the (limited) algorithm verification showed “method d” to deliver the right amount of correction (but this method has other drawbacks).

We then get for the signal S of pixel i in channel 1a:

$$S_{i\_1a}(\text{corrected}) = S_{i\_1a} - S_{k\_\text{stray}}(\text{sorted}) \qquad (2)$$

3.2 Correct seasonal variation in BSDF

This correction is based on the CHEOPS-GOME study of seasonal variability of the diffuser BSDF [R19]. The BSDF is described as polynomial function of solar azimuth angle on the diffuser.

Two approaches are presented in the study:

1. using a smoothed BSDF which is a 3rd order polynomial fit in wavelength; this is provided for all channels
2. a spectrally resolved BSDF, which can be provided for channels 1,3,4 but not for channel 2; this is because the frequent changes in etalon structure in channel 2 destroys the information in the analysis [R19]. As it may be that the spectral structure correlates with the detector etalon (although this is not obvious from the data) there may also be a real limitation for channel 2 here.

The CHEOPS-GOME study on diffuser BSDF [R19] proposes to fit the azimuth dependence with a polynomial. However, the data volume concerned is not a problem for the GDP extraction software. We can obtain a higher accuracy by using a look-up table (LUT) for a number of azimuth angles.

For the smoothed BSDF, the wavelength dependence for each azimuth angle is calculated as an N^{th} (default: 3^{rd}) order polynomial; the coefficients of this polynomial are in the LUT with dimensions (M, N+1) where the number of rows, M, is the number of azimuth angles.

For an azimuth angle $\alpha_{azi}(m)$, the smoothed BSDF as function of measurement wavelength λ_i is for each pixel i is given by:

$$BSDF(\lambda_i, \alpha_{azi}(m)) = \sum_{j=0}^{N} LUT_{mj} \cdot (\lambda_i - \lambda_c)^j \qquad (3)$$

where λ_c is a 'central wavelength' in the channel (to keep the numerical values of LUT_{mj} in a smaller range of magnitude).

For an azimuth angle $\alpha_{azi}(m) \le \alpha_{azi} \le \alpha_{azi}(m+1)$, the BSDF is calculated for table indices (m) and (m+1) and then linearly interpolated to α_{azi}.

For the spectrally resolved BSDF, a LUT is provided with dimensions (N_pix, M) where the number of columns, M, is the number of azimuth angles and N_pix is the number of pixels in a channel. The data are presented together with a grid of N_pix wavelengths λ_j. The processing is here:

1. calculate for the applicable azimuth angle the BSDF on the wavelength grid :

$$BSDF(\lambda_j, \alpha_{azi}(m)) = LUT_{jm} \qquad (4)$$

2. interpolate $BSDF(\lambda_j)$ to the wavelength grid of the measurement using Akima interpolation

For an azimuth angle $\alpha_{azi}(m) \le \alpha_{azi} \le \alpha_{azi}(m+1)$, the BSDF is calculated for table indices (m) and (m+1) and then linearly interpolated to α_{azi}.

As the analysis of the spectrally resolved BSDF has been limited to wavelength windows, one must accept a jump in level 1 radiances at the window edges after correction. Note that a similar principle is applied in the KNMI software [R17]. The current windows are: 250 - 312 nm, 315-

393 nm, 415-590 nm, 620-790 nm; perhaps this may be slightly enlarged in the final data set. Note, that the current windows cover all operationally retrieved trace gas species in the GDP. Also the ozone profile retrieval wavelengths used in this project are covered, with a possible exception in the 312-315 nm range (t.b.d.).

3.3 Correct degradation in reflectivity

The post-processing algorithm used by KNMI [R17] corrects the reflectivity (sun-normalised radiance) on the level 1 data on two levels:

1. A correction is made on the on-ground calibration of the BSDF (wavelength dependent correction, fixed in time)
2. A correction is made for time-dependent degradation of the BSDF (on the ratio of Radiance to Irradiance)

We have some reservations regarding the first correction, described in detail in [R16]. The recalibration of the BSDF is based on comparison of the level 1 measurements with Ozone profile retrievals at KNMI. However, the forward model used in the retrieval makes several assumptions regarding e.g. surface albedo (only relevant for $\lambda > 305$ nm), Ozone cross-sections, temperature profile, correction for polarisation in the scalar radiative transfer, ring effect. In general, this correction may more describe the errors in the forward modelling than the errors on the Level 1 data. We feel supported in this view by the fact that the correction does not improve the Ozone profile retrieval of other groups [R18].

We conclude that the “recalibration” of the on-ground BSDF from [R16] may be useable on the forward model used by KNMI, but should not be implemented as a general improvement of GOME level 1 data.

For the second correction we will use the results from the CHEOPS-GOME degradation study, which has been performed by SRON [R21].

The coefficients of the degradation will probably be available as a LUT for each channel. The first column of the LUT describes the date, subsequent columns provide for this date polynomial degradation coefficients as function of wavelength. The rows of the LUT contain the sequence of dates.

Let the LUT have dimensions (N+2,M). Let all counting start at 0. Application of this LUT is as follows.

1. The wavelength polynomial is of order N. The degradation for day t_m = LUT(0,m) as function of measurement wavelength λ_i is given for each pixel i by:

$$D(t_m, \lambda_i) = \sum_{n=0}^{N} LUT(n+1, m) \cdot \left(\frac{\lambda_i}{\lambda_{ref}}\right)^n \quad (5)$$

   For days between t_m and t_{m+1}, a linear interpolation is used between the degradations $D(t_m, \lambda_i)$ and $D(t_{m+1}, \lambda_i)$.

2. The level 1 earthshine radiances (not solar irradiance) for each day t are divided by the corresponding degradation $D(t, \lambda_i)$.

Note, that currently there is an option in the GDP extractor to apply degradation correction factors, derived from irradiance measurements, on both, radiances and irradiances. When this irradiance degradation is then applied on the reflectivity degradation, we get a radiance degradation. This is why D is applied on the radiance - although for calculation of the reflectivity one might also apply it on the BSDF instead.

3.4 Improvements of the polarisation correction algorithm

The PMDs measure polarisation for wavelengths $\lambda \geq 380$ nm. For shorter wavelengths, a theoretical model is required. Up to a wavelength $\lambda_{SS} \approx 300$ nm, the polarisation can be taken as constant and equal to the value for single scattering [R12]. In the GDP, the gap between these wavelength regions is bridged using a parameterisation given by the 'Generalised Distribution Function' (GDF):

$$F_1(\lambda) = \bar{P}(\bar{\lambda}) + \frac{w_0 \cdot \exp(-[\lambda - \lambda_{SS}] \cdot \beta)}{\{1 + \exp(-[\lambda - \lambda_{SS}] \cdot \beta)\}^2} \quad (6)$$

Here $\{\bar{P}, w0, \beta\}$ are parameters that characterise the GDF; they must be found to fit the given interpolation points. In the current GDP extraction software, λ_{SS} is taken as constant (300 nm) and the GDF is calculated up to a wavelength $\bar{\lambda} = 325$ nm. The value $\bar{P}(\bar{\lambda})$ is calculated in such a way that the GDF is continuous in gradient with a spline interpolation (Akima interpolation [R10]) through the PMD polarisation values.

The current GDP formulation has the drawback that $\bar{P}(\bar{\lambda})$ depends strongly on information from PMD-2 and PMD-3. However, the polarisation in the visible is physically decoupled from the polarisation in the UV and hence information is used which is not applicable. In the SCIAMACHY ATBD [R9], the GDF is initially connected to λ_A, the effective wavelength of PMD-1. Using the observation that the steepest gradient of the GDF is always near a fixed wavelength λ_m [R5], an analytical solution to the GDF parameters is possible [R9]. These are sequentially calculated using:

1. $\beta = (\ln(2 + \sqrt{3}))/(\lambda_m - \lambda_{SS})$
2. $\bar{P}(\bar{\lambda}) = (P_A - P_0 \cdot g_A(\beta))/(1 - g_A(\beta))$
3. $w_0 = 4 \cdot (P_0 - \bar{P}(\bar{\lambda}))$

   where P_0 is the theoretical polarisation at λ_{SS}, P_A is the polarisation of PMD-1, and $g_A(\beta)$ is an auxiliary function defined by:

$$g_A(\beta) = 4 \cdot \frac{\exp(-[\lambda_A - \lambda_{SS}] \cdot \beta)}{\{1 + \exp(-[\lambda_A - \lambda_{SS}] \cdot \beta)\}^2} \quad (7)$$

An improved algorithm has been proposed by Schutgens and Stammes [R14]. Here, λ_{SS} and λ_m are not fixed values, but they are parameterised as function of airmass, ground albedo and ozone content:

$$\lambda_{SS} = a_0 + \sum_{i=1}^{2} a_i/M^i + b_i \cdot \left(\frac{VCD}{VCD_0} - 1\right)^i \quad (8)$$

$$\lambda_m = \sum_{i=0}^{2}\sum_{j=0}^{2} c_{ij}/M^i \cdot A^j + \sum_{i=1}^{2} d_i \cdot \left(\frac{VCD}{VCD_0} - 1\right)^i \quad (9)$$

where M is the airmass, A is the surface albedo, and VCD is the vertical ozone column [DU]; VCD_0 = 345.8 DU.

The parameters have been fitted from model calculations as:

```
a = [ 308.68, -29.10, 11.46 ]
b = [     0.,   7.58, -4.26 ]
    [316.43, -41.89, 29.49 ]
c = [  0.33,  -0.06,  0.66 ]
    [ -1.11,   0.56, -3.46 ]
```

where index i runs over column and index j over row

```
d = [0., 7.20, -4.08 ]
```

In the KNMI algorithm [R17], this parameterisation has been implemented using the Fortuyn-Kelder ozone climatology [R13] to calculate *VCD*, whereas the albedo is calculated by comparing the measured GOME reflectance at 380 nm with a pre-calculated lookup table. We propose to follow this implementation here.

An improvement may be made in the airmass calculation. In Ref. [R14], [R17] the formula for the plane-parallel case is used. This limits the calculation to solar zenith angles SZA < 85^{o}. We use a formula for spherical geometry from H. Eskes (private communication):

$$M = \frac{1}{\cos(VZA)} + \frac{\sqrt{\cos(SZA)^2 + (h/R)^2 + 2(h/R)} - \cos(SZA)}{h/R} \qquad (10)$$

where *VZA* is the nadir viewing angle, h is the top of atmosphere height, and R is the Earth radius. This formula gives physical results for the airmass even for SZA > 90^{o}, although the numerical values then become strongly dependent on the assumed top of atmosphere height. We will use $h = 60$ and $R = 6300$.

The parameters *a-d* in the equations above have been calculated for SZA < 75^{o} and 220 < *VCD* < 440. We find that using our airmass calculation, these parameters still yield plausible results for SZA < 95^{o} and 100 < *VCD* < 600 DU. There are thus no practical limitations in applying the parameters in the GDP software.

Reference [R14] provides parameterisations of λ_{SS} and λ_m, but does not mention how the value of $\bar{P}(\bar{\lambda})$ has to be obtained, or how the GDF has to be connected to the PMD polarisation points. In the KNMI algorithm, the GDF parameters are calculated as above, i.e. the GDF is connected to the point (λ_A ,P_A). The parameterisation is then used between λ_{SS} and $\bar{\lambda} = 325$ and Akima interpolation is used from $\bar{\lambda} = 325$ onwards.

The GDF is a slowly decreasing function for wavelengths above ~320 nm. Using it up to 325 nm therefore prescribes a rather flat function, and a continuous connection in gradient forces also the Akima interpolation to be pretty flat until the polarisation point from PMD-1. This behaviour is not always supported by simulations of polarisation, especially above clear surfaces with low albedo (high polarisation). Here polarisation shows a local minimum near 320 nm (depending on airmass) and a local maximum near 400-450 nm.

We prefer to use the method from the SCIAMACHY ATBD [R9]. Here, the GDF parameterisation is only used between λ_{SS} and a wavelength ($\lambda_0+\Delta\lambda_{GDF}$) which is chosen such that it falls still in the strongly descending part of the GDF. Continuation in gradient will force it to follow the GDF further downwards as would the parameterisation do, but it gives the algorithm a bit more freedom to shape the curve according to the gradient obtained from PMD measurements around

λ_A. In that sense it is a bit of an intermediate between the current GDP algorithm and the prescription of a spectrally flat function. A difference with the current GDP algorithm is that the GDF parameters are not *determined* by all PMD measurements: they are determined only by the theoretical polarisation and the measurement of PMD-1, but the polarisation curve can smoothly shape itself between $(\lambda_0 + \Delta\lambda_{GDF})$ and λ_A using the gradient between PMD-1 and PMD-2. To keep close to the GomeCal approach, we will use a value of $\Delta\lambda_{GDF}$ = 25 nm; this yields on average a connecting point near 325 nm.

A limitation needs to be implemented against using unphysical polarisation values from PMD-1. Unphysical are polarisation fractions where the Stokes fraction *Q/I* of the theoretical point is smaller than, or has a different sign as, the one from PMD-1. These are given by the conditions:

$$|P_0 - 0{,}5| < |P_A - 0{,}5| \qquad (11)$$

$$(P_0 - 0{,}5) \cdot (P_A - 0{,}5) < 0 \qquad (12)$$

Analysis of GOME PMD-1 data has shown that, on average, the degree of polarisation at PMD-1 is half that of the theoretical single scatter value.

In case of unphysical PMD-1 values, replace P_A by this statistical value:

$$P_A \rightarrow 0{,}5 \cdot (1 - \Delta + 2\Delta \cdot P_0) \qquad (13)$$

with $\Delta = 0{,}5$

For the purpose of Ozone profile retrieval, it is sufficient to consider only the polarisation up to the effective wavelength of PMD-1 (~380 nm).

One may consider in the GDP extraction software to apply Equations (11) and (12) also to the p-values of PMD-2 and PMD-3. The statistical depolarisation is here given by $\Delta = 0{,}35$ and $\Delta = 0{,}2$, respectively. However, in this case it may be more apt to relate the depolarisation not to the theoretical value, but to the measured value provided by PMD-1:

$$P \rightarrow 0{,}5 \cdot (1 - \Delta' + 2\Delta' \cdot P_A) \qquad (14)$$

with $\Delta' = 0{,}75$ and $\Delta' = 0{,}4$ for PMD-2 and PMD-3, respectively.

Note, that a completely different algorithm for the retrieval of polarisation has been proposed [R15]. Here, also spectral structure of polarisation in the Huggins bands and in (Fraunhofer) absorption lines is modeled. Based on radiative transfer modeling, it claims to reduce the radiance calibration errors due to polarisation sensitivity from the current (using the new GDF parameterisation) 1% level to below the 0.1% level. However, without proper corrections (only partially implemented in their method so far) significant overcorrection may take place in strong absorption lines. Since this employs a radical new method, which apparently still needs some fine-tuning, and whose implications for e.g. DOAS trace gas fitting have not been investigated, it falls out of the scope of the current project.

4 References

[R1] Burrows, J. P., K. Chance, P. Crutzen, et al., SCIAMACHY A European proposal for atmospheric remote sensing from the ESA polar platform, Max- Planck Institut fuer Chemie, Mainz, Germany, 1988

[R2] Burrows J.P., Chance K.V., "SCIAMACHY and GOME: the scientific objectives", in: Optical Methods in Atmospheric Chemistry, SPIE Vol. 1715, 1992

[R3] GOME Interim Science Report, by Burrows J. P., K. V. Chance, A. P. H. Goede, R. Guzzi, B. J. Kerridge, C. Muller, D. Perner, U. Platt, J.-P. Pommereau, W. Schneider, R. J. Spurr, H. van der Woerd, edited by T. D. Guyenne and C. J. Readings, SP-1151, ESA publications Division, ESTEC, Noordwijk, The Netherlands, ISBN 92-9092-041-6 (1993)

[R4] GOME Users Manual, ESA SP-1182, ESA/ESTEC, Noordwijk, The Netherlands (1996)

[R5] GOME Level 0 to 1b Algorithm Description, ER-TN-DLR-GO-0022, Issue 4/A, DLR, August 1996.

[R6] GOME Data Processor - Update Report for GDP 0-to-1 Version 2.0 and GDP 1-to-2 Version 2.7, ER-TN-DLR-GO-0043, Issue 1/A, DLR, 24.8.1999

[R7] GOME Data Processor - Extraction Software User's Manual, ER-SUM-DLR-GO-0045, Issue 2, DLR, 5.8.2002

[R8] GDAQI - Final Report, TN-GDAQI-003SR/2000, SRON, September 2000

[R9] SCIAMACHY Level 0 to 1c Processing - Algorithm Theoretical Basis Document, ENV-ATB-DLR-SCIA-0041, Issue 2, DLR, 14.12.2001

[R10] Hiroshi Akima, "A new method of interpolation and smooth curve fitting based on local procedures", J. ACM, Vol. 17(4), 1970, 589-602

[R11] Jochen Stutz and Ulrich Platt, "Problems in using diode arrays for open path DOAS measurements of atmospheric species", Institut für Umweltphysik, Universität Heidelberg

[R12] Piet Stammes, "The seventh point polarisation algorithm, Internal Report" (GOME and SCIAMACHY Data & Algorithm group), KNMI De Bilt, 1994

[R13] Fortuin, J.P.F. and Kelder, H.M."An ozone climatology based on ozonezonde and satellite measurements," J. Geophys. Res. 103, p.31,709, 1998

[R14] N.A.J. Schutgens, P. Stammes, "Parametrisation of earth's polarisation spectrum from 290 to 330 nm", J.Quant.Spectr.Rad.Transf. 75, p.239, 2002

[R15] N.A.J. Schutgens, P. Stammes, "A novel approach to the polaraisation correction of spaceborne spectrometers", J. Geophys. Res. 108 (D7), doi 10.1029/2002JD002736, 2002

[R16] R. van der A, "Recalibration of GOME spectra for the purpose of ozone profile retrieval", KNMI Technical Report TR-236, 26.6.2001

[R17] J.H.G.M. van Geffen, "Documentation of the software packeage GomeCal (Version 1.0)", KNMI Technical Report TR-255, 2003

[R18] B. Kerridge, private communication, April 2004

[R19] S. Slijkhuis, "Study on Seasonal Effects on the ERS-2/GOME Diffuser BSDF", DLR report CH-TN-DLR-GO-0001, Issue 1, 9.5.2004

[R20] S. Slijkhuis, "Study on Correction of Signal Background on the ERS-2/GOME Level 1 data", DLR report CH-TN-DLR-GO-0002, Issue 1, 3.9.2004

[R21] J.M. Krijger, I Aben, J. Landgraf, "GOME: scan-mirror degradation correction", ESA Atm.Sci.Conf. , May 2006, in press